Immunosensing Microchip Using Fast and Selective Preparation of an Iridium Oxide Nanoparticle-Based Pseudoreference Electrode

Md. Abdul Aziz,[a] *Byung-Kwon Kim*,[a] *Minjung Kim*,[b] *Sang-Youn Yang*,[a] *Hyun-Woo Lee*,[a] *Sang Woo Han*,[b] *Yeong Il Kim*,[c] *Sangyong Jon*,[d] *Haesik Yang**[a]

[a] Department of Chemistry and Chemistry Institute of Functional Materials, Pusan National University, Busan 609-735, Korea
[b] Department of Chemistry and KI for the NanoCentury, KAIST, Daejeon 305-701, Korea
[c] Department of Chemistry, Pukyong National University, Busan 608-737, Korea
[d] Department of Life Science, Gwangju Institute of Science and Technology, Gwangju 500-712, Korea
*e-mail: hyang@pusan.ac.kr

Received: March 30, 2011
Accepted: May 2, 2011

Abstract
Iridium oxide (IrO_x) electrodes have been used as pseudoreference electrodes operating in buffered solutions, but their preparation requires a time-consuming procedure. Here we report a simple, fast, and selective preparation of an IrO_x pseudoreference electrode based on the deposition of presynthesized IrO_x nanoparticles. The reference electrode is applied to an immunosensing microchip consisting of a patterned poly(dimethylsiloxane) plate and an indium–tin oxide-micropatterned glass. The sequence of microfabrication is optimized to accomplish better performance. The microchip is operated by capillary-driven microfluidic controls and used for detecting a target mouse IgG. The measured detection limit in the microchip is ca. 10 pg/mL.

Keywords: Reference electrodes, Iridium oxide, Carbon nanotubes, Immunosensors, Microchips

DOI: 10.1002/elan.201100184

1 Introduction

Microchip-based biosensors that use small sample volumes have been widely developed for use in point-of-care testing [1,2]. Of many detection methods, electrochemical methods match well with biosensors, as they are sensitive and even small electrochemical instruments allow reproducible and accurate potential (or current) application and measurement for a long time without calibration [3–7]. However, reproducibility and accuracy of the electrochemical biosensors is strongly dependent on the performance of microfabricated reference electrodes along with sensing working electrodes. For practical application, it is essential to microfabricate stable and reproducible reference and sensing electrodes in a simple manner.

Miniature Ag/AgCl electrodes have commonly been employed as microfabricated reference electrodes because of their high exchange currents and stable electrode potentials [8–11]. However, easy dissolution of AgCl in high Cl^- concentrations and a complicated fabrication procedure of Ag/AgCl films limits their reliable and practical use. To improve the stability of Ag/AgCl reference electrodes, their surfaces should be covered with polymer membranes [12–14]. Alternatively, miniature iridium oxide (IrO_x)- and platinum oxide-modified electrodes have been used as pseudoreference electrodes operating in buffered solutions, as their electrode potentials are stable in the solutions [15–19]. Formation of IrO_x electrodes has been based on electrochemical deposition of iridium ion [15,20,21], electrochemical oxidation of iridium metal [22,23], sputtered coating [24], and thermal method [25,26]. The electrochemical methods require prolonged repeated potential cycling (and complicated procedures for preparing iridium ion solutions), and other methods require vacuum condition or high temperature. This calls for a simpler preparation method that can be reliably applied to microchip-based biosensors. Monodisperse IrO_x nanoparticles can be readily prepared in aqueous solutions, and they show good electrochemical performance [27,28]. If an electrode is simply modified with IrO_x nanoparticles, the modified electrode might be used as a reference electrode.

Microfabrication of microchip-based biosensors accompanies many selective surface modifications that significantly influence the overall biosensor performance. In particular, the microfabrication process of reference electrodes can have a detrimental effect on prefabricated working electrodes, and vice versa. Thus, the sequence of microfabrication processes as well as selective modification methods are of great importance in obtaining better biosensor performance. Moreover, in biosensors all surfa-

ces in contact with a solution should be protein-resistant in order to obtain low background levels.

In recent years, the authors have developed a sensitive electrochemical immunosensor based on the formation of a partial monolayer of carboxylated carbon nanotube (CNT) on indium–tin oxide (ITO) electrodes [29]. Avidin and poly(ethylene glycol) (PEG)-silane copolymer were used for antibody immobilization and low levels of nonspecific binding. The authors have also developed microchips employing capillary-driven microfluidic controls in order to take advantage of simple spontaneous fluidic control [11,30].

In this study, we present a microchip-based immunosensor that employs an IrO_x nanoparticle-modified electrode as a pseudoreference electrode. The microchip consists of an upper plate made of poly(dimethylsiloxane) (PDMS) and a lower plate made of an ITO-micropatterned glass. The reference and sensing electrodes are formed on the ITO micropatterns with selective surface modification. The sequence of microfabrication is optimized to accomplish better performance of reference and sensing electrodes. The microchip is operated by capillary-driven microfluidic controls and used for detecting a target mouse IgG.

2 Experimental

2.1 Chemicals

Multiwalled CNT, K_2IrCl_6, sodium hydrogen citrate, trichloroethylene, H_2O_2, NH_4OH, avidin, biotinylated goat antimouse IgG, mouse IgG from serum, and alkaline phosphatase (ALP)-conjugated goat antimouse IgG were purchased from Sigma-Aldrich. 4-Aminophenyl phosphate monosodium salt hydrate (APP), skim milk powder, and absolute ethanol were obtained from Biosynth, Fluka, and Fisher Scientific, respectively. Sylgard 184A and sylgard 184B were obtained from Dow Corning. All buffer reagents and other inorganic chemicals were supplied by Sigma-Aldrich, unless otherwise stated. All aqueous solutions were prepared in doubly distilled water.

The phosphate buffered saline (PBS) solution consisted of 0.01 M phosphate, 0.138 M NaCl, and 0.0027 M KCl (pH 7.4). The PBSB solution contained all the ingredients of PBS with additional 1 % (w/v) albumin-bovine serum (pH 7.4). The rinsing buffer (RB) solution was prepared using 50 mM tromethamine, 40 mM HCl, 0.5 M NaCl, and 0.05 % (w/v) albumin-bovine serum (pH 7.6). The

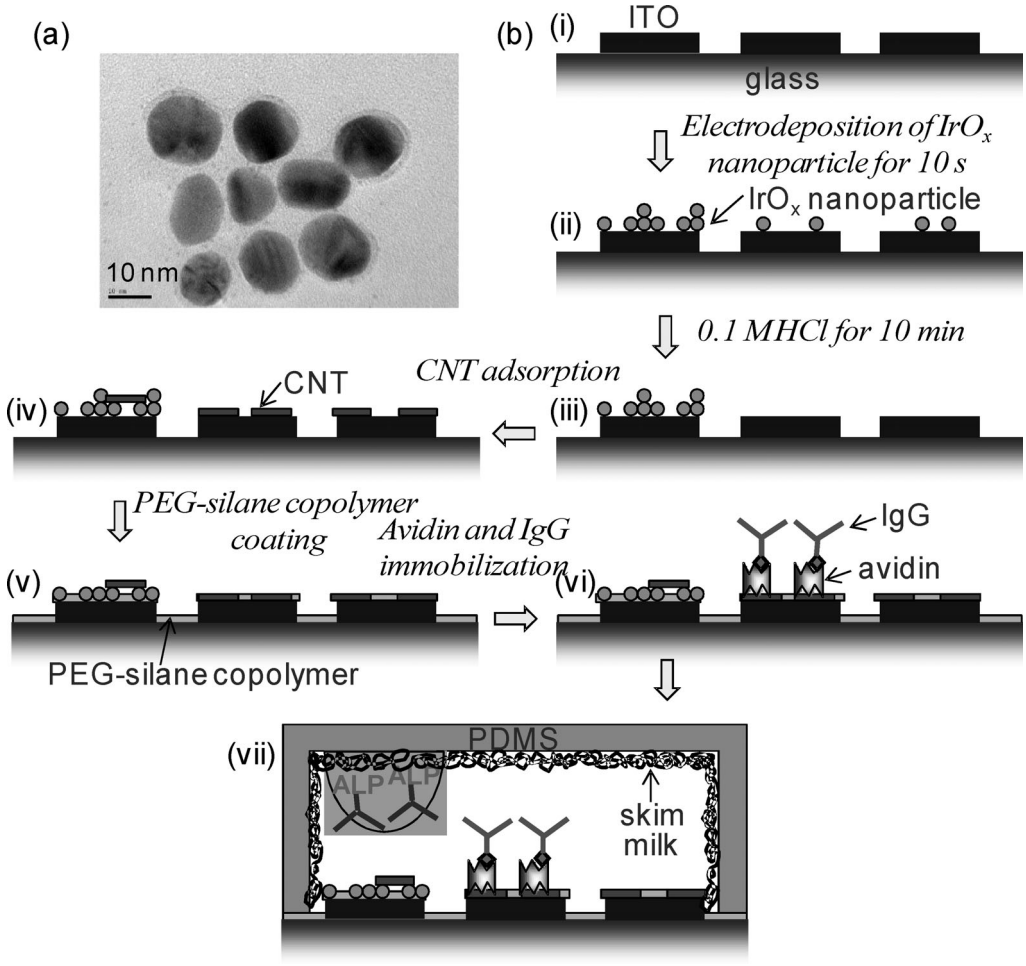

Fig. 1. a) TEM image of IrO_x nanoparticles. b) Schematic diagram for the sequence of microchip microfabrication.

Tris buffer solution for the electrochemical experiment consisted of 50 mM tromethamine, 10 mM KCl, 10.5 mM $MgCl_2$, and 7 mM HCl (pH 9.0).

Carboxylated multiwalled CNTs were prepared according to our previous report [29]. IrO_x nanoparticles were synthesized by hydrolysis of $IrCl_6^-$ in the presence of citrate by following a previous report [20]. The nanoparticle diameter was ca. 14 ± 2 nm (Figure 1a). The nanoparticle solution showed a characteristic broad absorption band at 591 nm. PEG-silane copolymer was synthesized as previously reported [29].

2.2 Fabrication of the Lower Plate

ITO-coated glasses were obtained from Samsung Corning (Daegu, Korea). ITO micropatterns on a glass substrate were fabricated via standard photolithography and etching processes as reported previously [11]. The patterned ITO glass substrate was diced into smaller plates (2.0×1.0 cm each). Each plate contained three micropatterned ITO electrodes (electrode area = ca. 0.20 mm^2 for a working electrode; ca. 0.52 mm^2 for a reference and a counter electrode). The micropatterned plates were successively cleaned with trichloroethylene, ethanol, and water with 15-min ultrasonication, followed by drying at 50 °C. The cleaned plates were pretreated in a mixture of 5:1:1 H_2O/H_2O_2 (30%)/NH_4OH (30%) (v/v/v) at 70 °C for 1.5 h. The plates were then washed with copious amounts of water and dried at 50 °C for 20 min. Afterward, the synthesized IrO_x nanoparticles were galvanostatically deposited on one of three micropatterned ITO electrodes (Figure 1b-ii). Galvanostatic deposition was performed by applying a constant current of 200 μA. After washing with water, the plate was immersed in 0.1 M HCl to remove adsorbed IrO_x nanoparticles from other two electrodes (Figure 1b-iii). After washing with water and drying at 50 °C, the plate was immersed in an aqueous solution of 1 mg/mL carboxylated multiwalled CNT for 4 h to immobilize CNT, followed by washing with water and drying at 50 °C (Figure 1b-iv). The plate was immersed in a methanol solution containing 10 mg/mL PEG-silane copolymer for 2 h, and then washed with methanol, followed by curing at 50 °C for 30 min (Figure 1b-v). The plate was immersed for 6 h in a PBS solution containing 100 μg/mL avidin and then washed twice with PBS. Afterward, the avidin-coated electrodes were immersed in a PBSB solution containing 0.05% (v/v) Tween-20 for 30 min to prevent nonspecific adsorption of proteins, followed by washing with RB and drying with nitrogen. 5 μL of a PBSB solution containing 10 μg/mL biotinylated goat antimouse IgG was dropped on the working electrode for 30 min, followed by washing with RB and drying with nitrogen gas (Figure 1b-vi). The final plate was used as a lower plate of an immunosensing microchip (Figure 1b-vii).

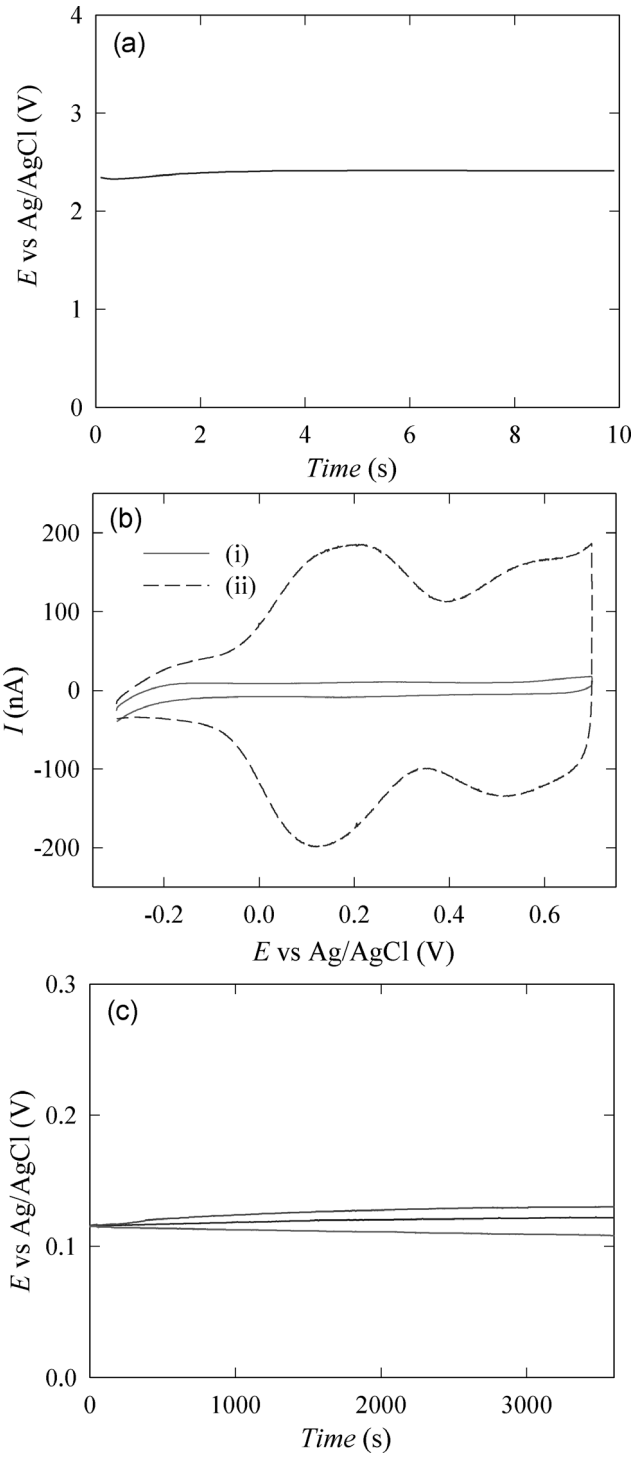

Fig. 2. a) Potential change during the galvanostatic deposition of IrO_x nanoparticles at a constant current of 200 μA. b) Cyclic voltammograms recorded (at a scan rate of 20 mV/s) at two ITO electrodes in PBS after the immersion in 0.1 M HCl for 10 min. Curve i is for an undeposited ITO electrode, and curve ii for a galvanostatically IrO_x nanoparticle-deposited ITO electrode. c) Open-circuit potential of three IrO_x nanoparticle-based pseudoreference electrodes measured in PBS.

2.3 Fabrication of the Upper Plate

A master for a patterned PDMS plate was fabricated as reported previously [11]. A mixed solution of sylgard 184A and sylgard 184B (10 : 1 by mass) were poured into the patterned master, and the trapped air bubbles were removed by vacuum pump. Subsequently, the solution was cured at 65 °C for 2 h for cross-linking. After separating from the master, the patterned PDMS substrate was cut into patterned PDMS plates. The measured plate thickness was 2.0 mm, and the channel depth was ca. 105 μm. Two solution inlets with 2.0-mm diameter and an air vent with 1.0-mm diameter were formed on the patterned PDMS plate using a puncher. The PDMS plate was immersed in an aqueous solution of 0.1 g/mL skim milk for 2 h to cover the whole surface with skim milk, followed by washing with water. 1 μL of a PBSB solution containing 10 μg/mL ALP-conjugated antimouse IgG was then dropped inside a reaction chamber of the PDMS plate. This PDMS plate was used as an upper plate of a microchip. Finally, the upper and the lower plate were assembled by pressing (Figure 1b-vii).

2.4 Operation of the Immunosensing Microchip

3.5 μL of PBSB containing different concentrations of mouse IgG were injected into the sample solution inlet of the immunosensing microchip. After 10-min incubation, 10 μL of Tris buffer containing 4 mM APP were injected into the washing solution inlet. After 20-min incubation, a cyclic voltammogram were recorded using a potentiostat (CHI 617B, CH instruments) at room temperature.

3 Results and Discussion

3.1 Optimization of the Sequence of Microfabrication

Three ITO micropatterns on a glass plate were used for preparing working, reference, and counter electrodes. In order to obtain selective surface modification, the ITO-micropatterned plate should be immersed in a solution or only one electrode should be exposed to a solution by dropping. The immersing method is simple but can cause contamination of the other two ITO electrodes and the glass surface, whereas the dropping method is good for selective modification but can cause less reproducible results. In this study, both the immersing and the dropping method were employed: most of the construction process was based on the immersing method, and only the final construction of an immunosensing layer on the working electrode was based on the dropping method.

Bare ITO electrodes show low electrocatalytic activities, requiring modification with any electrocatalytic material when they are used as working and counter electrodes. In our previous study, the simple modification of ITO electrodes with a partial monolayer of carboxylated

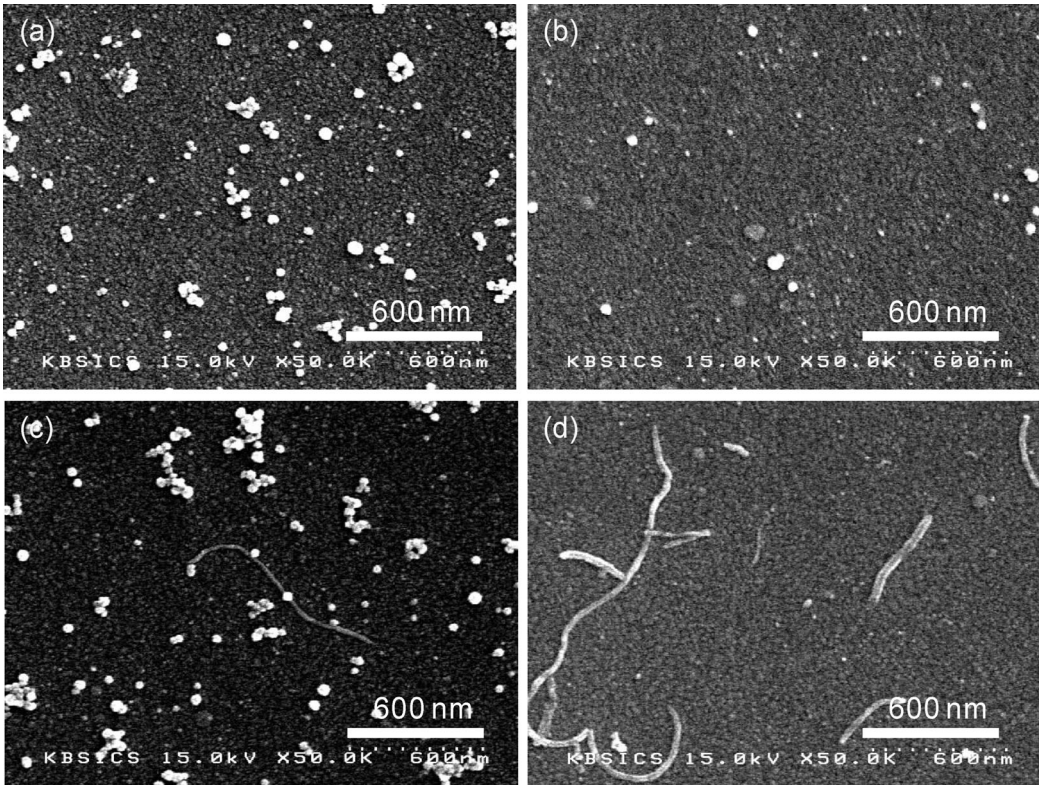

Fig. 3. SEM images of (a, c) a galvanostatically IrO_x-deposited ITO electrode and (b, d) an undeposited ITO electrode, (a, b) before and (c, d) after immersion in 0.1 M HCl for 10 min and afterwars in an aqueous solution of 1 mg/mL carboxylated multiwalled CNT for 4 h.

CNTs signficantly improved their electrocatalytic activities [29]. In this study, the immersion of an ITO-micropatterned plate into an aqueous solution containing carboxylated CNT allowed simultaneous modification of three micropatterned ITO electrodes with CNT. Thus prepared ITO electrodes were used as working and counter electrodes. However, it was impossible to achieve reproducible modification of IrO_x nanoparticles on CNT-modified ITO electrodes. Thus, the modification of one electrode with IrO_x nanoparticles was performed prior to the modification with CNT. Microfabrication processes of reference electrodes can give a detrimental effect on sensing working electrodes. For this reason, the immunosensing layer was constructed after the reference electrode was prepared.

Yagi et al. reported that IrO_x nanoparticles can be readily adsorbed on ITO electrodes [28]. However, such adsoprtion made it difficult to accomplish selective modification of IrO_x nanoparticle on one ITO micropattern. Moreover, the amount of adsorbed IrO_x nanoparticles were not high enough to allow high exchange currents, and the adsorbed nanoparticles were easily desorbed. For the formation of a layer of IrO_x nanoparticles, a short galvanostatic deposition was employed (Figure 1b-ii). Figure 2a shows the potential change during galvanostatic deposition for 10 s. This short deposition minimized the adsoption of IrO_x nanoparticles on the other two electrodes. Figures 3a and 3b show SEM images of a galvanostatically IrO_x nanoparticle-deposited ITO electrode and an undeposited ITO electrode, respectively. Many IrO_x nanoparticles were observed on the deposited electrode (Figure 3a), whereas the number of nanoparticles were much less on the undeposited electrode (Figure 3b). The adsorbed IrO_x nanoparticles on the undeposited electrode (i.e., working electrode) could cause unwanted redox currents of IrO_x, resulting in high levels of background currents. Thus, these nanoparticles had to be removed before the immunosensing layer was constructed.

To remove the adsorbed IrO_x nanoparticles, the plate was immersed in 0.1 M HCl for 10 min (Figure 1b-iii). Figure 2b shows cyclic voltammograms recorded at two ITO electrodes after immersion. In the case of the IrO_x nanoparticle-deposited ITO electrode, a typical redox behavior of IrO_x was observed (curve ii of Figure 2b). As for the undeposited electrode, a redox peak related to the redox reaction of IrO_x was not observed (curve i of Figure 2b). These results indicate that most of the galvanostatically deposited IrO_x nanoparticles remained on ITO electrodes and that most of the adsorbed IrO_x nanoparticles were desorbed from ITO electrodes.

After carrying out selective modification of IrO_x nanoparticles, the ITO-micropatterned plate was immersed in a solution of carboxylated CNT (Figure 1b-iv). Figures 3c and 3d show SEM images of the IrO_x nanoparticle-deposited electrode and the undeposited electrode, respectively, obtained after the CNT adsorption. CNTs were randomly adsorbed with a partial monolayer (Figure 3d). CNT adsorption on the IrO_x nanoparticle-deposited electrode was not much (Figure 3c). Importantly, most of the IrO_x nanoparticles still remained on ITO electrodes.

3.2 Performance of IrO_x Nanoparticle-Based Pseudoreference Electrodes

In curve ii of Figure 2b, the anodic peak at ca. 0.2 V corresponds to the oxidation of Ir_2O_3 to IrO_2, and the cathodic peak at ca. 0.1 V corresponds to the reduction of IrO_2 to Ir_2O_3. This cyclic voltammetric behavior is well in accord with those of previously reported IrO_x electrodes that allowed stable electrode potentials in buffered solutions [31]. Generally, other methods for preparing IrO_x electrodes require prolonged repeated potential cycling (and a complicated procedure for preparing iridium ion solutions) [15–18]. In the case of IrO_x nanoparticle-based deposition, IrO_x nanoparticles that possess the characteristics required for a pseudoreference electrode were presynthesized in large quantities, and were then deposited on a specific electrode in a short time. This method significantly reduced the time to prepare IrO_x electrodes.

Figure 2c shows the change in open-circuit potential with time for three IrO_x nanoparticle-modified electrodes in PBS (pH 7.4). The potential drift was less than 15 mV for 1 h, indicating that the electrode potentials of three pseudoreference electrodes are quite stable. The potential

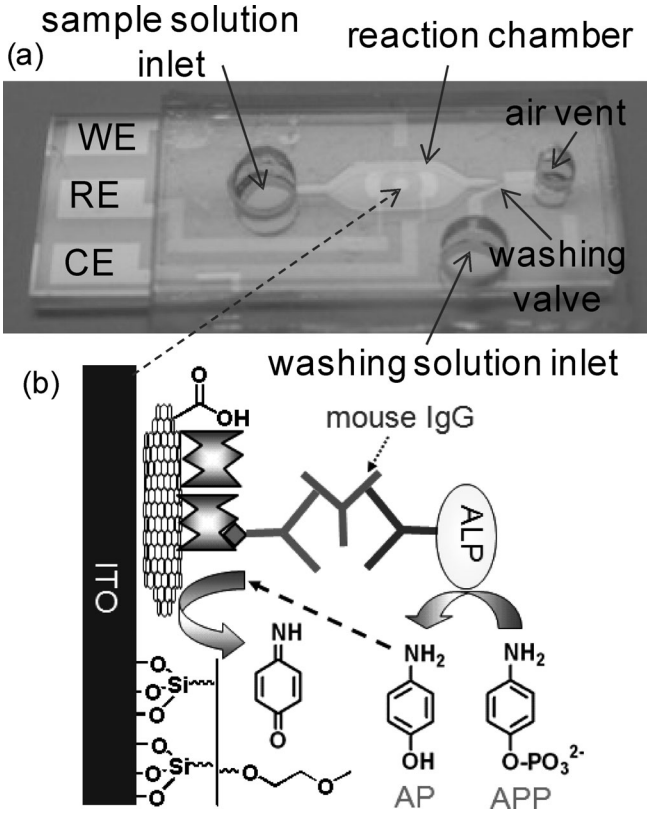

Fig. 4. a) Photograph of an immunosensing microchip. b) Schematic diagram of an electrochemical immunosensor for detecting mouse IgG. WE, RE, and CE represent working electrode, reference electrode, and counter electrode, respectively.

difference between the three electrodes was also less than 22 mV.

When the galvanostatic deposition of IrO_x nanoparticles was performed for longer times, thicker IrO_x films were obtained. However, the unwanted adsorption of IrO_x nanoparticles on the other ITO electrodes was considerable, and it was difficult to fully remove the adsorbed nanoparticles although they were readily desorbed.

3.3 Microchip-Based Immunosensing

Figure 4a shows a photograph of a microchip for detecting a target mouse IgG. The microfluidic control in the microchip was described in our previous report [11]. In brief, a sample solution containing target mouse IgG was injected into the sample solution inlet. The reaction chamber was filled with the solution by capillarity, up to the washing valve that acts as a capillary-pressure barrier [30]. In the reaction chamber, the ALP-conjugated antimouse IgG adsorbed on the upper PDMS plate (Figure 1b-vii) was dissolved into the solution. For 10 min, mouse IgG bound to the ALP-conjugated antimouse IgG and the complex then bound to the biotinylated antimouse IgG on the working electrode. Afterward, a washing solution containing APP was loaded from the washing solution inlet. When the washing solution merged with the sample solution at the washing valve, a solution flow from the washing solution inlet to the sample solution inlet was generated due to the inlet-pressure difference between the two inlets. The solution flow induced the replacement of the sample solution by the washing solution. The unbound ALP-conjugated IgG was washed out from the reaction chamber. The solution flow lasted until the two inlet pressures equilibrated. The bound ALP enzyme on the working electrode converted APP into AP. After an incubation time of 20 min, the generated AP was electrochemically measured. The CNT on the ITO electrode allowed fast electrochemical oxidation of AP.

Figures 5a–c show cyclic voltammograms recorded in different concentrations of mouse IgG. The anodic currents above ca. 0.1 V during the anodic scan are mainly due to the electrooxidation of AP, while the cathodic currents below ca. 0.1 V are due to the electroreduction of *p*-

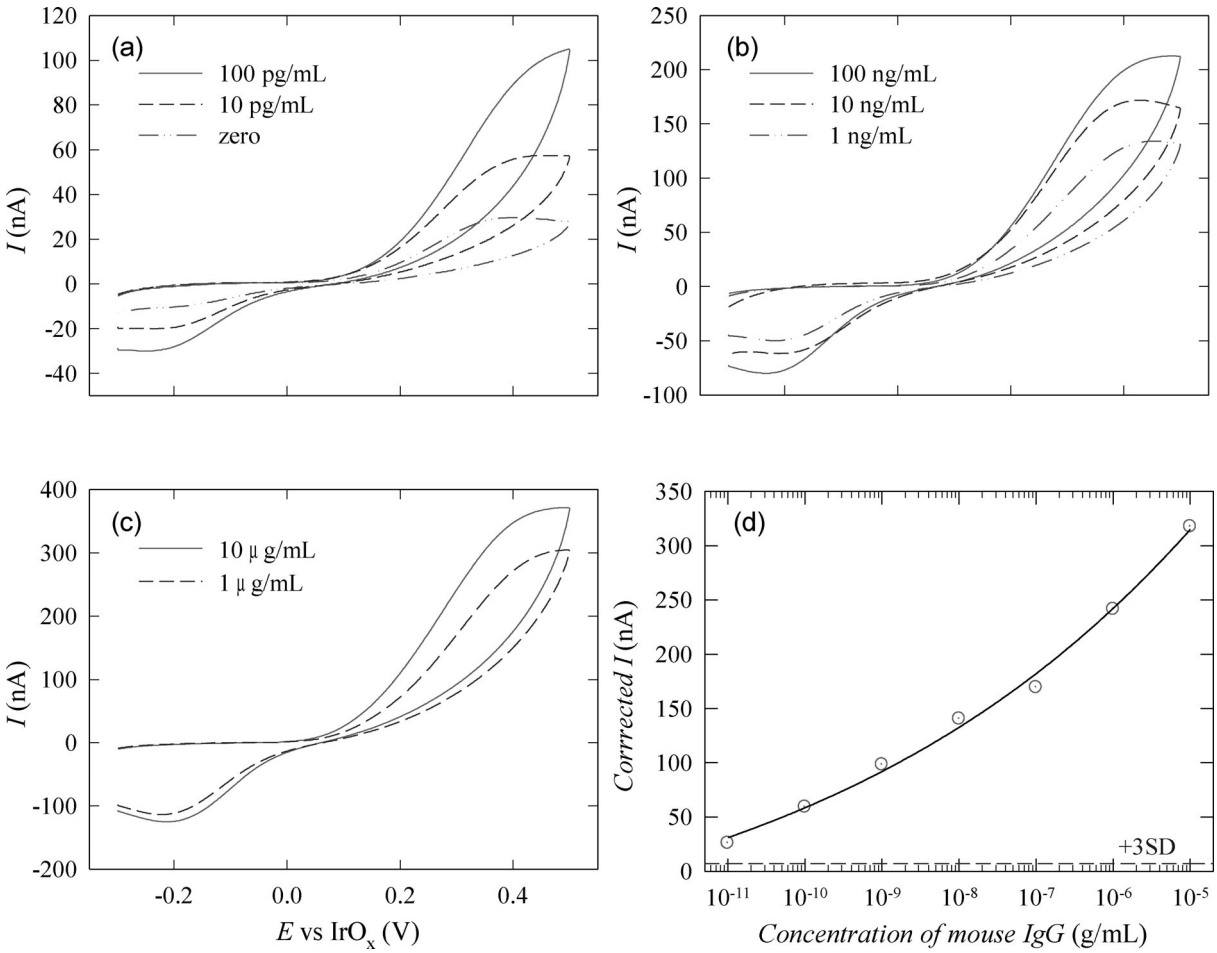

Fig. 5. a–c) Dependence of cyclic voltammograms on the concentration of mouse IgG. The cyclic voltammograms were obtained at a scan rate of 20 mV/s with immunosensing microchips. d) Calibration plot for the immunosensor. All current data obtained at 0.40 V were subtracted by the mean current at zero concentration. The dashed line corresponds to three times the standard deviation (*SD*) at zero concentration.

quinoneimine. As the concentration of mouse IgG increased, the anodic currents increased because the amount of bound ALP-conjugated IgG increased. Figure 5d represents a calibration plot for the immunosensor. The calculated detection limit was ca. 10 pg/mL, which was similar to that obtained with large ITO electrodes [29]. This low detection limit indicates that the reference and working electrodes were reproducibly prepared and operated and that the nonspecific binding of ALP-conjugated antimouse IgG was not substantial in the reaction chamber of the microchip.

4 Conclusions

We have developed a simple, fast, and selective preparation method of an IrO_x nanoparticle-based pseudoreference electrode. This method significantly reduced the preparation time of IrO_x electrodes. In the microchip, CNT-modified ITO electrodes were used as working and counter electrodes, and the enzyme-based electrochemical detection was combined with capillary-driven microfluidic control. The reference and working electrodes were reproducibly prepared and operated, and the nonspecific binding of ALP-conjugated antimouse IgG was not substantial. These results allowed us to obtain a very low detection limit of 10 pg/mL in the microchip.

Acknowledgements

This research was supported by the Public Welfare & Safety Research Program (2010-0020772), the Basic Science Research Program (2009-0085182) and the Nano/Bio Science & Technology Program (2005-01333) through the *National Research Foundation of Korea* (*NRF*) funded by the *Ministry of Education, Science and Technology.*

References

[1] A. H. C. Ng, U. Uddayasankar, A. R. Wheeler, *Anal. Bioanal. Chem.* **2010**, *397*, 991.
[2] A. Bange, H. B. Halsall, W. R. Heineman, *Biosen. Bioelectron.* **2005**, *20*, 2488.
[3] J. Wang, *Electroanalysis* **2005**, *17*, 1133.
[4] J. Wang, M. Pumera, M. P. Chatrathi, A. Rodriguez, S. Spillman, R. S. Martin, S. M. Lunte, *Electroanalysis* **2002**, *14*, 1251.
[5] M. Pumera, A. Merkoçi, S. Alegret, *Trends Anal. Chem.* **2006**, *25*, 219.
[6] M. Mir, A. Homs, J. Samitier, *Electrophoresis* **2009**, *30*, 3386.
[7] X. Xu, S. Zhang, H. Chen, J. Kong, *Talanta* **2009**, *80*, 8.
[8] H. Suzuki, H. Shiroishi, S. Sasaki, I. Karube, *Anal. Chem.* **1999**, *71*, 5069.
[9] B. J. Polk, A. S. Stelzenmuller, G. Mijares, W. MacCrehan, M. Gaitan, *Sens. Actuators B* **2006**, *114*, 239.
[10] A. Hiratsuka, K. Ikebukuro, I. Karube, K. Kojima, H. Suzuki, H. Muguruma, *Analyst* **2001**, *126*, 658.
[11] B.-K. Kim, S.-Y. Yang, M. A. Aziz, K. Jo, D. Sung, S. Jon, H. Y. Woo, H. Yang, *Electroanalysis* **2010**, *22*, 2235.
[12] F. Moussy, D. J. Harrison, *Anal. Chem.* **1994**, *66*, 674.
[13] J. Ha, S. M. Martin, Y. Jeon, I. J. Yoon, R. B. Brown, H. Nam, G. S. Cha, *Anal. Chim. Acta* **2005**, *549*, 59.
[14] I.-Y. Huang, R.-S. Huang, L.-H. Lo, *Sens. Actuators B* **2003**, *94*, 53.
[15] H. Yang, S. K. Kang, C. A. Choi, H. Kim, D.-H. Shin, Y. S. Kim, Y. T. Kim, *Lab Chip* **2010**, *4*, 42.
[16] C. Li, C. H. Ahn, L. A. Shutter, R. K. Narayan, *Biosens. Bioelectron.* **2009**, *25*, 173.
[17] M. Odijk, A. Baumann, W. Olthuis, A. van den Berg, U. Karst, *Biosens. Bioelectron.* **2010**, *26*, 1521.
[18] I. A. Ges, B. L. Ivanov, A. A. Werdich, F. J. Baudenbacher, *Biosens. Bioelectron.* **2007**, *22*, 1303.
[19] J.-H. Han, S. Park, H. Boo, H. C. Kim, J. Nho, T. D. Chung, *Electroanalysis* **2007**, *19*, 786.
[20] S. A. M. Marzouk, S. Ufer, R. P. Buck, T. A. Johnson, L. A. Dunlap, W. E. Cascio, *Anal. Chem.* **1998**, *70*, 5054.
[21] S. A. M. Marzouk, *Anal. Chem.* **2003**, *75*, 1258.
[22] S. Yao, M. Wang, M. Madou, *J. Electrochem. Soc.* **2001**, *148*, H29.
[23] E. E.-D. M. El-Giar, D. O. Wipf, *J. Electroanal. Chem.* **2007**, *609*, 147.
[24] T. Katsube, I. Lauks, J. N. Zemel, *Sens. Actuators* **1982**, *2*, 399.
[25] M. L. Hitchman, S. Ramanathan, *Talanta* **1992**, *39*, 137.
[26] K. Kinoshita, M. J. Madou, *J. Electrochem. Soc.* **1984**, *131*, 1089.
[27] M. Hara, C. C. Waraksa, J. T. Lean, B. A. Lewis, T. E. Mallouk, *J. Phys. Chem. A* **2000**, *104*, 5275.
[28] M. Yagi, E. Tomita, S. Sakita, T. Kuwabara, K. Nagai, *J. Phys. Chem. B* **2005**, *109*, 21489.
[29] M. A. Aziz, S. Park, S. Jon, H. Yang, *Chem. Commun.* **2007**, 2610.
[30] B.-K. Kim, S.-J. Kim, S.-Y. Yang, H. Yang, *J. Micromech. Microeng.* **2007**, *17*, N22.
[31] S. Carroll, R. P. Baldwin, *Anal. Chem.* **2010**, *82*, 878.

